

RESEARCH ARTICLE

CHANGES IN FIRE SEVERITY ACROSS GRADIENTS OF CLIMATE, FIRE SIZE, AND TOPOGRAPHY: A LANDSCAPE ECOLOGICAL PERSPECTIVE

Sandra L. Haire* and Kevin McGarigal

University of Massachusetts, Department of Natural Resources Conservation,
160 Holdsworth Way, Amherst, Massachusetts 01003-9285, USA

*Corresponding author: Tel.: 001-413-387-5413; e-mail: shaire@nrc.umass.edu

ABSTRACT

Fire events contribute to landscape pattern at multiple spatial and temporal scales, and a landscape perspective can provide relevant information for assessing how a changing fire regime will influence pattern-process dynamics. We investigated how the amount and spatial arrangement of high-severity patches varied among 20 fires that occurred in Arizona and New Mexico, USA, across gradients in fire size and climate. The climate gradient was based on the Multivariate El Niño Southern Oscillation Index. In the southwestern US, cool dry conditions are prevalent in La Niña at one extreme, and at the other end, warm wet conditions occur in El Niño. Fires were generally larger in La Niña climates; however, several fires deviated from this trend. Moreover, some spatial properties of severity did not correspond to fire size or to changes in climate. Within the nine largest fires, we analyzed the influence of landscape characteristics defined by topographic discontinuity on spatial patterns of fire severity. Characteristics of topography altered spatial patterns of severity at some places within all the nine fires, and we identified thresholds where small changes in terrain resulted in dramatic effects on severity. From a management perspective, consideration of the spatial configuration of severely burned areas can help qualify judgments based on fire size or severity composition alone by linking pattern to ecological processes of interest. Furthermore, examination of individual fire events could lead to identification of climate contexts in which fires can meet management objectives for sustainable forests.

Keywords: Arizona, climate change, fire severity, forest fire ecology, Generalized Additive Models, New Mexico, ponderosa pine, southwestern USA, spatial pattern metrics, topographic gradients

Citation: Haire, S.L., and K. McGarigal. 2009. Changes in fire severity across gradients of climate, fire size, and topography: a landscape ecological perspective. *Fire Ecology* 5(2): 86-103.

INTRODUCTION

Fire events contribute to landscape pattern at multiple spatial and temporal scales (White and Pickett 1985). Determining the effects of a

particular event is contingent upon understanding the spatial heterogeneity of landscape pattern, the way spatial pattern changes through time, and the traits of species and communities that determine critical thresholds for dramatic

shifts in composition and function (Romme *et al.* 1998). Studies of ecosystems across the western US suggest that climate conditions are altering the extent and severity of fires (Grissino-Mayer and Swetnam 2000, Westerling *et al.* 2006, Littell *et al.* 2009). A landscape ecological perspective can provide relevant information for assessing how this changing fire regime will influence pattern-process dynamics in systems where equilibrium conditions are unlikely (Pickett *et al.* 1992).

In forested ecosystems of Arizona and New Mexico, USA, some recent fires are larger and more severe (i.e., include extensive areas of tree mortality) than those documented historically (but see Whitlock 2004 and Margolis *et al.* 2007). Past studies in other regions have demonstrated that larger fire size can be accompanied by increased severity; however, size and configuration of burn patterns generate highly heterogeneous landscapes in many cases (Collins *et al.* 2007, Lutz *et al.* 2009). Large fire events exhibit a wide range of ecological responses, and impact does not always increase with extent (Romme *et al.* 1998).

The first objective of our research was to learn how spatial patterns of severity change across gradients of fire size and climate. We examined a set of fires that occurred in northern Arizona and New Mexico, where extensive surface and stand-replacing fires have been associated with severe drought (Grissino-Mayer and Swetnam 2000, Margolis *et al.* 2007) linked to the El Niño Southern Oscillation (Swetnam and Betancourt 1998). The characteristics of individual fires hold important implications for ecosystem change at broad scales, but more local processes, including plant succession, respond to spatial heterogeneity at finer scales within a fire event. In particular, the spatial patterns of biological legacies strongly influence regeneration of ponderosa pine (*Pinus ponderosa* C. Lawson) and other plants that are limited by dispersal abilities, while other life history strategies can be successful under a

wider range of landscape configurations (Haire and McGarigal 2008). Landscape patterns, including topographic and physiographic features, can influence behavior of fire, resulting in greater heterogeneity of fire severity (Turner and Romme 1994, Baker 2003).

Thus, our second objective was to determine how local landscape patterns of topography influenced severity within fires that burned under different climates. Following the model developed by Turner and Romme (1994), we expected terrain effects to be predominant during moderate climate conditions; in extreme conditions, high landscape connectivity of fuels (e.g., from either continuous fuels or high winds) would lead to severe fire even in rugged terrain. In addition, we used a flexible modeling approach to identify thresholds where severity decreased or increased across a gradient in topography complexity. Previous studies of topographic effects on fire have focused on burn probability (Miller *et al.* 2008), fire behavior and spread (Rothermel 1983, Yang *et al.* 2008) and fire occurrence (Kellogg *et al.* 2008, Stambaugh and Guyette 2008). Our study focuses on the spatial heterogeneity of fire severity as a response to changes in topography.

METHODS

We selected 20 fires from databases developed and maintained by the Santa Fe National Forest, New Mexico; Bandelier National Monument, New Mexico; Kaibab National Forest, Arizona; and Grand Canyon National Park, Arizona (Figure 1; Table 1). The criteria for inclusion were: 1) size >100 ha; 2) ponderosa pine forest comprised a portion of pre-fire cover types; and 3) available aerial photography, satellite images, and field data were sufficient to map fire severity. We identified and mapped four older fires (pre-1980) that fit these criteria, five New Mexico fires that burned in 1996 to 2000, and 11 Arizona fires that occurred in 1996 to 2004 (Table 1). Without considering limita-

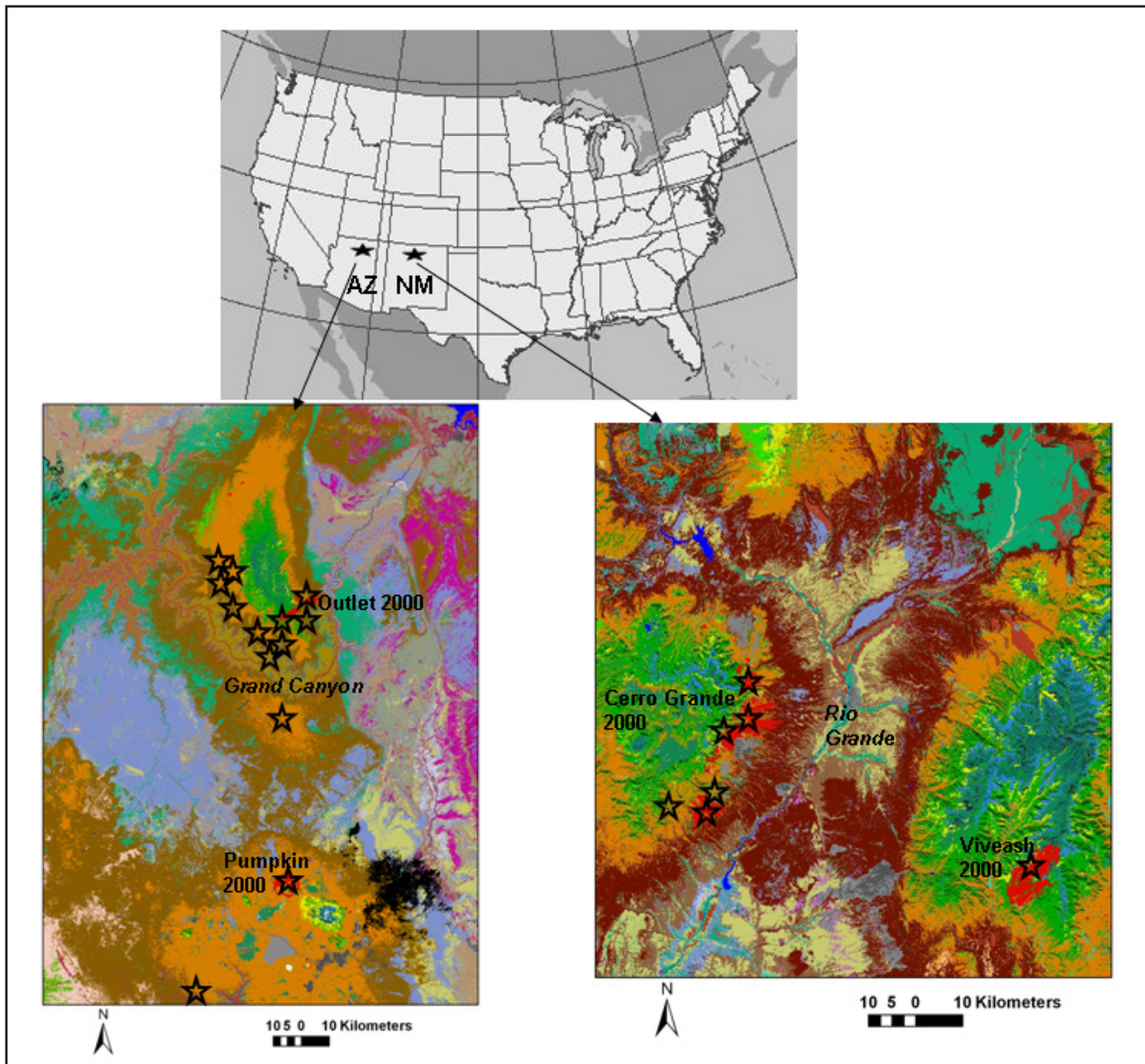


Figure 1. Approximate location of study areas (stars) in Arizona and New Mexico, USA, displayed on landcover data from the Southwest Gap Analysis (<http://fws-nmcfwru.nmsu.edu/swregap/>). Some recent fires were specifically mapped (shaded in red) and firenames for 2000 are labeled on the figure. In New Mexico, stars in a general north-south direction correspond to: Oso 1998, Cerro Grande 2000, American Springs 1951, La Mesa 1977, Dome 1996, and Nicole 1996 (west of Dome). Viveash is east of the Rio Grande Valley, which flows north to south in north central New Mexico. Arizona fires south of the Grand Canyon are: Long Jim 2004, Pumpkin 2000, and Summit to the southwest. On the north rim of the Grand Canyon, Outlet 2000, Saddle Mountain 1960, Outlet 2004, Vista 2001, Bright 2004, and Walhalla 2004 are grouped together. The group of stars farther north represents approximate locations for Quartz 2004, Swamp Ridge 2001, Tower 2001, and Poplar-Big-Rose 2003. Ponderosa pine forests are shaded orange; conifer forests with mixed composition are green; piñon-juniper (*Pinus edulis*-*Juniperus* spp.) woodlands are brown.

tions imposed by availability of remotely sensed and field data, the 16 recent fires represented 22.5% of the eligible fires ($n = 71$) in the Forest Service and National Park Service databases. The recent fires included a range of sizes, from

relatively small (e.g., the Nicole and Summit fires were less than 200 ha) up to the largest fire in the aforementioned time periods, the Cerro Grande Fire, which was 17 349 ha.

Table 1. Fires included in the study, the total area burned, date of detection, and MEI calculated for the detection month and the 18 mo pre-fire interval. The table is sorted by the 18 mo mean. The largest fires ($n = 9$) were included in the within-fires analysis and are marked with an asterisk.

Fire name	Location ¹	Total area (ha)	Detection date (Yr.JulianDate)	MEI month of detection	18-month mean
*Cerro Grande	SFNF NM	17349.39	2000.125	-0.34	-0.88
*Outlet 2000	GRCA AZ	4804.74	2000.131	-0.34	-0.88
*Pumpkin	KNF AZ	6383.79	2000.146	0.03	-0.81
*Viveash	SFNF NM	8811.09	2000.151	0.03	-0.81
Swamp Ridge	GRCA AZ	1295.01	2001.229	0.29	-0.28
Tower	GRCA AZ	1683.00	2001.241	0.29	-0.28
*Saddle Mountain	KNF AZ	3931.74	1960.173	-0.26	0.00
Nicole	SFNF NM	158.58	1996.175	-0.01	0.02
American Springs	SFNF NM	703.26	1954.157	-1.55	0.03
*Dome	SFNF NM	6648.57	1996.116	-0.49	0.04
*La Mesa	BAND NM	5745.60	1977.167	0.49	0.06
Walhalla	GRCA AZ	1325.16	2004.259	0.56	0.32
Bright	GRCA AZ	520.20	2004.237	0.61	0.34
Outlet 2004	GRCA AZ	450.27	2004.236	0.61	0.34
Quartz	GRCA AZ	228.96	2004.222	0.46	0.35
Long Jim	GRCA AZ	820.80	2004.126	0.27	0.48
*Poplar-Big-Rose	GRCA AZ	6839.10	2003.190	0.00	0.58
*Oso	SFNF NM	2462.67	1998.182	1.14	1.75

¹ Location codes (one of potentially multiple management agencies): KNF = Kaibab National Forest, SFNF = Santa Fe National Forest, GRCA = Grand Canyon National Park, BAND = Bandelier National Monument, AZ = Arizona, NM = New Mexico.

We determined the occurrence of ponderosa pine forests within burned areas using data from the Southwest Gap Analysis (<http://fws-nmcfwru.nmsu.edu/swregap/>) and local land management databases (i.e., Kaibab and Santa Fe national forests, Bandelier National Monument, and Grand Canyon National Park). Especially in the case of larger fires, the burned area encompassed a gradient of forest types that generally corresponded with changes in elevation. At the lowest elevations, piñon-juniper (*Pinus edulis* Engelm.-*Juniperus* spp. L.) woodlands were common; ponderosa pine forests appeared as elevation increased. At the highest elevations, forests were composed of two or more species including ponderosa pine, Douglas-fir (*Pseudotsuga menziesii* [Mirb.]

Franco), white fir (*Abies concolor* [Gord. & Glend.] Lindl. ex Hildebr.), Englemann spruce (*Picea englemanni* Parry ex Engelm.), and quaking aspen (*Populus tremuloides* Michx.).

We obtained aerial photography of sufficient quality to distinguish recently burned areas for the four older fires (dates ranged from 2 yr to 6 yr post-fire; scale varied from 1:600 to 1:24 000). High severity was defined as areas with complete tree mortality, identified when charred soil or other blackened surfaces, and when standing or down dead trees were visible in forest openings. All other areas were classified as lower severity, and could include low, moderate, or mixed effects, as well as unburned islands within the fire perimeter. We validated classification of high-severity areas

using pre-fire photos in conjunction with field studies at La Mesa and Saddle Mountain fires (Haire and McGarigal 2008); for the American Springs and Summit fires, we reviewed maps with local managers.

All but two of the recent fires had burn severity maps available through the National Park Service and US Geological Survey Burn Severity Mapping Project (2007). For these two fires (Nicole Fire 1996 and Dome Fire 1996), we acquired Landsat images made available by Burn Severity Mapping Project managers, and followed the image processing methodology (Key and Benson 2005) using ERDAS Imagine (Leica Geosystems Geospatial Imaging, Norcross, Georgia, USA). Burn severity was defined as a gradient of change based on a normalized index of Landsat bands 4 and 7, calculated using images collected within one or two years before and after the fire event (i.e., extended assessment; Key 2006). The post-fire index subtracted from the pre-fire index produces the differenced Normalized Burn Ratio (dNBR), which can be used as a continuous measure of severity, or classified to relate to field conditions reflecting severity.

We chose to classify the dNBR to match the aerial photo interpretation of older burns with dates preceding satellite image availability. To that end, we examined aerial photography taken in 2002 and 2005 at random points to classify areas of severe burn for the Oso, Dome, and Nicole fires. For all other fires, we used available field data, either collected with FIREMON methodology (i.e., Composite Burn Index, Key and Benson 2005), or with a method that applied a comparable rating of severity (N.B. Kotliar, US Geological Survey, unpublished data), all collected within two years post-burn. We performed a classification tree analysis (De'ath and Fabricius 2000) to determine thresholds of dNBR image values for the field and random point high-severity and low-severity classes. The dNBR value, as well

as its variance and mean in a 3×3 grid cell window (30 m resolution) around the random point or field plot center, were included as predictors in the classification trees. Minimum sample size for field or random point data was 40, and overall classification accuracy was $\geq 89\%$ across all fires.

Metrics used to quantify spatial heterogeneity reflected the two elements of landscape structure: composition (the relative amount of what is present) and configuration (the arrangement of spatial attributes on the landscape) (Turner *et al.* 2001, McGarigal *et al.* 2002). Our goal was to represent several variations on spatial configuration including aggregation at the cell (AI, CLUMPY) and patch (DIVISION) level. Core area (CAI_AM) was included because of its reflection of both patch shape and size (Table 2). We defined increased severity by lower values for patch division and greater values for the remaining metrics. Our definition assumes that configuration of biological legacies, including seed sources, would be more scattered as configurations of high-severity patches became more contiguous, with larger patch sizes and more areas located far from an edge of lower severity. The spatial pattern metrics were calculated for each of the 20 fires (among-fires scale) and within a moving window that varied in size (within-fires scale: 500 m, 250 m, and 125 m radius) for the nine largest fires using FRAGSTATS (McGarigal *et al.* 2002). The 20 fires occurred in varied climate contexts across the Multivariate El Niño Southern Oscillation Index (MEI) gradient (National Oceanic and Atmospheric Administration 2009), and the large size of the nine fires provided wide variability in topography.

At the among-fires scale, we derived several climate indices using the MEI. In the southern Rocky Mountains, El Niño years are characterized by wetter than average winter and spring, followed by drier than average La Niña years, in a 2 yr to 6 yr cycle. The MEI is a multivariate measure of the El Niño South-

Table 2. FRAGSTATS spatial pattern metrics chosen to quantify attributes of fire severity, with their abbreviations and descriptions (McGarigal *et al.* 2002).

Spatial pattern metric	Description
PLAND	Percent of the Landscape: proportional abundance of high-severity patches in the burned landscape; severity composition.
AREA_AM	Area-weighted mean patch size: the proportional area of each high-severity patch, based on total area of all high-severity patches.
AI	Aggregation Index: the number of adjacencies between high-severity cells, divided by the maximum possible number of adjacencies (0% to 100%). Equals 0 when there are no like adjacencies and 100 when all cells form a single, compact patch.
CLUMPY	Clumpiness Index: the proportion of adjacencies of high-severity cells, scaled to reflect its deviation from that expected under a spatially random distribution, facilitating comparison of high-severity cell aggregation among landscapes (range -1 to 1).
DIVISION	Division Index: based on the cumulative patch area distribution, DIVISION is the probability that two randomly chosen cells are not situated in the same high-severity patch (0 to 1). The value approaches 1 as the proportion of the landscape comprised of high severity decreases and as high-severity patches decrease in size.
CAI_AM	Core Area Index (Area-weighted Mean): percentage of the high-severity patch that is greater than 100 m from an edge of lower severity, summed for all high-severity patches. The index is scaled relative to proportional abundance of high-severity patches to enable comparison among landscapes.

ern Oscillation signal, where negative values correspond to La Niña and positive values are associated with El Niño periods. The MEI is based on the first principal component of sea-level pressure, surface zonal and meridional wind components, sea surface temperature, and cloudiness observed over the tropical Pacific (Wolter and Timlin 1998). The recorded monthly value (MEI) is an average of the principal component for the preceding two months. We derived climate indices by averaging the MEI at nine intervals preceding the detection date of each fire (i.e., 6, 12, 18, 24, 30, 36, 42, 48, and 54 months prior), as well as by determining the MEI value for the month in which each fire was detected (Table 1).

We used Generalized Additive Models (GAMs; Wood 2006) to explore relationships in the data. Ecological data often exhibit variations across environmental gradients (Guisan *et al.* 2002); therefore, we chose a flexible modeling approach. Generalized Additive

Models were advantageous for our purpose because the solutions are data-driven and can range from simple linear (parametric) fits to highly complex smooths that require greater degrees of freedom for each term. We used the “mgcv” library implementation of GAMs (The R Project for Statistical Computing, <http://www.r-project.org>), in which smoothing parameters are chosen to minimize a generalized cross-validation score, and overly complex models are prevented by a penalty imposed during maximum likelihood estimation (Wood 2006). The models take the form

$$[\textit{severity}_i] = f_i(x_i),$$

where the response was a severity metric (e.g., PLAND; Table 2), f was a smooth term, and x was either MEI or fire size (among-fires scale) or topographic complexity (within-fires scale). The smooth of x was plotted along with its 95% confidence limit to explore patterns in the data.

First, at the among-fires scale, we determined which of the MEI-derived indices had the best linear correlation to fire size. Then we modeled the relationship, using GAMs, between a) fire size and the best (most correlated) climate index, b) severity pattern metrics and fire size, and c) severity pattern metrics and the best climate index. When relationships were extremely variable at this scale, we increased the penalty for complexity in the smoothing parameter, which reduces wiggleness and thereby emphasizes general trends.

At the within-fires scale, we developed GAMs to quantify changes in severity across gradients of topographic discontinuity (hereafter synonymous with complexity or heterogeneity). Topographic complexity was modeled by calculating the variance of elevation values (1 min National Elevation Dataset; US Geological Survey 1999) within the moving windows using the focal function in ArcInfo (Environmental Systems Research Institute, Redlands, California, USA). Using all of the moving window grids (severity and topographic discontinuity at three scales), we generated a random sample of grid cell values proportional to fire size for (GAM) modeling purposes (far-left column, Table 3). We evaluated the GAMs at each moving window scale to determine at what scale patterns of topography and severity were most related, and focused our interpretation on the scale with the greatest number of significant smooth terms ($P \leq 0.001$) out of 54 models (i.e., 6 metrics \times 9 fires). To aid interpretation of results, we identified landforms that defined topographic variability at each fire using maps from local land managers, US Geological Survey topographic quads, and knowledge we acquired during site visits.

RESULTS

Among-Fires Scale: Twenty Fires

Fire size was related to the MEI gradient; the greatest linear correlation was with the

MEI 18 month mean (Pearson's $r = -0.50$). This relationship was somewhat weaker without the Cerro Grande Fire ($r = -0.39$), but generally held for all intervals up to and including 24 months. Intervals further out from the fire date had little correlation to fire size (Pearson's r ranged from -0.15 to 0.15). The GAM smooth curve exhibited a significant decrease across the 18 month mean (Figure 2; $P = 0.02$, deviance explained = 41.4%). The confidence interval at the El Niño end was wide, due to the single fire at that end of the climate gradient (Oso Fire 1998). Two relatively large fires occurred midway along the gradient (Dome Fire 1996 and Poplar-Big-Rose Fire 2003). The Cerro Grande Fire of 2000 influenced the trend at the extreme La Niña end of the scale because of its outstanding size (17 349 ha; Table 1 and Figure 2).

Trends in severity were related to fire size in some cases, but models were weaker than that of fire size and climate. We set a significance threshold of $P < 0.2$ so that we could present some examples of variability in severity among fires (Figure 3). Composition of high severity (PLAND), area-weighted mean patch size (AREA_AM), and core area index (CAI_AM) generally increased with the total area burned. However, Cerro Grande, the largest fire, had a lower value for PLAND than some of the smaller fires, which resulted in a downward turn in the smooth curve. Another exception to the overall trend was the Saddle Mountain Fire, which was composed of 49% high severity: an outstandingly large value for a fire that burned less than 5000 ha. Its area-weighted mean patch size (AREA_AM) was an extreme value on the size gradient as well (Figure 3). Cell aggregation (CLUMPY) exhibited high variability in smaller fires, and consistently high values in intermediate and large sizes. The Quartz Fire of 2004 had extremely low cell aggregation compared to the other fires (CLUMPY = -0.63), indicating that its high-severity burned area was strongly disaggregated.

Table 3. Results of the within-fire analysis for the nine largest fires, summarized for the 500 m radius window scale. Random sample of grid cells within each fire was chosen proportional to fire size. The description of climate context was based on MEI values and identification of major shifts in MEI (see Figure 5). Background geographic information describes the landforms that define topographic variability at each site.

Fire name (sample size)	Pattern metric	Deviance explained (%)	MEI date of detection	MEI 18 mo mean	Climate context/geographic considerations
Cerro Grande 2000 (n = 3500)	PLAND	0.24	-0.34	-0.88	Burned in drought conditions that followed the 1997/98 El Niño. Homogeneous topography occurred primarily at low to mid- elevations, with increased heterogeneity at mesa-canyon interfaces and as elevation increased.
	AI	0.17			
	AREA_AM	0.18			
	CAI_AM	0.20			
	DIVISION	0.14			
	CLUMPY	0.01			
Outlet 2000 (n = 1000)	PLAND	0.26	-0.34	-0.88	Burned in drought conditions that followed the 1997/98 El Niño. Relatively little variation in topography on the Kaibab Plateau north of the Grand Canyon.
	AI	0.18			
	AREA_AM	0.25			
	CAI_AM	0.29			
	DIVISION	0.23			
	CLUMPY	0.02			
Pumpkin 2000 (n = 1300)	PLAND	0.10	0.03	-0.81	Burned in less dry conditions, but still within the drought that followed the 1997/98 El Niño. Burned on and around Kendrick Peak, part of the San Francisco Mountains volcanic field. Greatest variance in elevation occurred at highest elevation, where very steep slopes are located.
	AI	0.05			
	AREA_AM	0.08			
	CAI_AM	0.11			
	DIVISION	0.08			
	CLUMPY	0.03			
Viveash 2000 (n = 1800)	PLAND	0.09	0.03	-0.81	Burned in less dry conditions, but still within the drought that followed the 1997/98 El Niño. Network of streams and especially the Pecos River associated with dramatic shifts in topography. Steep mountains, located in the southern end of the Sangre de Cristo Mountains.
	AI	0.09			
	AREA_AM	0.06			
	CAI_AM	0.04			
	DIVISION	0.05			
	CLUMPY	0.05			
Saddle Mountain 1960 (n = 800)	PLAND	0.12	-0.26	0.00	Followed a spike in El Niño (1958-1960) and occurred near the beginning of a negative trend in MEI (i.e., more droughty conditions). The topography creates dramatic relief; high variability occurs where steep scarp slopes, or combs, are adjacent to narrow stream bottoms, and near sheer walls on the south that form the Nankowep Rim.
	AI	0.07			
	AREA_AM	0.15			
	CAI_AM	0.07			
	DIVISION	0.14			
	CLUMPY	0.04			
Dome 1996 (n = 1350)	PLAND	0.24	-0.49	0.04	Situated in a drought that immediately followed a wetter, El Niño period (ca. 1990-1995). Topographic shifts defined by alternating broad mesas and steep canyons. Capulin Canyon and San Miguel Mountains are areas with the most heterogeneous topography.
	AI	0.09			
	AREA_AM	0.21			
	CAI_AM	0.05			
	DIVISION	0.20			
	CLUMPY	0.00			
La Mesa 1977 (n = 1150)	PLAND	0.21	0.49	0.06	Burned during El Niño and was preceded by an extreme drought (ca. 1974-1976). Topographic variability most dramatic at the edges of steep canyons (Frijoles and Alamo) and broad mesas that define the Pajarito Plateau.
	AI	0.07			
	AREA_AM	0.14			
	CAI_AM	0.05			
	DIVISION	0.15			
	CLUMPY	0.11			
Poplar-Big- Rose 2003 (n = 1400)	PLAND	0.05	0.00	0.58	Occurred during an El Niño phase that began in late 2001-2002. Low topographic complexity on this high-elevation plateau, with some variability around streams and one area of high variability at the edge of the Grand Canyon of the Colorado River.
	AI	0.07			
	AREA_AM	0.05			
	CAI_AM	0.06			
	DIVISION	0.05			
	CLUMPY	0.04			
Oso 1998 (n = 500)	PLAND	0.55	1.14	1.75	Occurred during and was preceded by the historic El Niño of 1997/98. Greatest topographic heterogeneity where broad mesas meet steep canyons, most notably the Santa Clara Canyon.
	AI	0.29			
	AREA_AM	0.62			
	CAI_AM	0.64			
	DIVISION	0.68			
	CLUMPY	0.17			

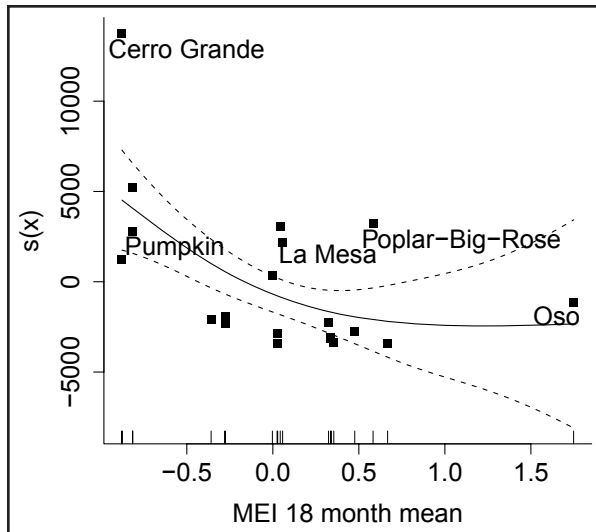


Figure 2. The plot of the GAM smooth function for fire size in relation to the MEI 18 month mean, with residuals for the 20 fires; the y-axis is scaled by the smooth function of x . Dotted lines are 95% confidence intervals. Fire name labels are located at the lower right of the residual of interest, with the exception of Oso. Fire size generally decreased across the pre-burn mean MEI, where negative x -axis values correspond to 18 mo pre-burn time periods that were dominated by La Niña.

Severity patterns corresponded to the climate gradient in only two cases: AREA_AM and CAI_AM ($P < 0.2$; Figure 4). These measures of severity tended to be greater at the La Niña end of the climate scale. The Oso Fire, however, had relatively high core area index for an El Niño fire. Values of greater magnitude for these metrics midway along the gradient, exemplified by Saddle Mountain Fire, were contrary to the overall trend.

Within-Fires Scale: Nine Fires

Severity had the strongest relationship to topographic heterogeneity at the broadest measured scale, based on GAMs. The number of significant smooth terms ($P < 0.001$) was greatest at the 500 m scale (52 out of 54); less than half of the GAMs had significant smooth terms at the 125 m and 250 m scales. At the 500 m scale, models for Oso Fire had the best fit, with topographic heterogeneity explaining up to 68% deviance (Oso DIVISION; Table

3). Cerro Grande, Outlet, Dome, and La Mesa fires had at least one model with $\geq 20\%$ deviance explained. Models for Pumpkin, Viveash, Saddle Mountain, and Poplar-Big-Rose fires were poorer; most explained $< 10\%$ deviance.

The climate context for a majority of fires was defined by drought conditions during La Niña years preceded by a wetter El Niño period (Table 3; Figure 5). These fires included the four fires in year 2000, Saddle Mountain (1960), and Dome (1996). The context of two fires placed them in more moderate climate scenarios: La Mesa Fire, which occurred in El Niño but was preceded by a multiple-year drought, and Poplar-Big-Rose, which occurred in and was preceded by El Niño. The Oso Fire of 1998 was the only burn situated within an extreme El Niño event.

A variety of landforms influenced topographic variability at the fires. Greatest variance in elevation at Cerro Grande, Dome, La Mesa, and Oso was associated with the interface of steep canyons and broad mesas that characterize their region of occurrence in northern New Mexico (Table 3). In addition, the extremely large area burned by Cerro Grande encompassed homogeneous topography at lower elevations and more variable topography as elevation increased.

The Arizona fires with the most similar topography were Outlet and Poplar-Big-Rose, which were located on the Kaibab Plateau, north of the Grand Canyon. Streams were the main source of variation in topography at both of these sites, which were otherwise fairly homogeneous. Pumpkin and Viveash were in unique situations compared to other fires; Pumpkin burned Kendrick Mountain, which is part of the San Francisco Mountains volcanic field, and Viveash is at the southern end of the Sangre de Cristo Mountains. Topographic variability at both Pumpkin and Viveash increased due to very steep slopes; at Viveash, rivers and streams were also associated with complex patterns of topography. Saddle Mountain was another unique case, where

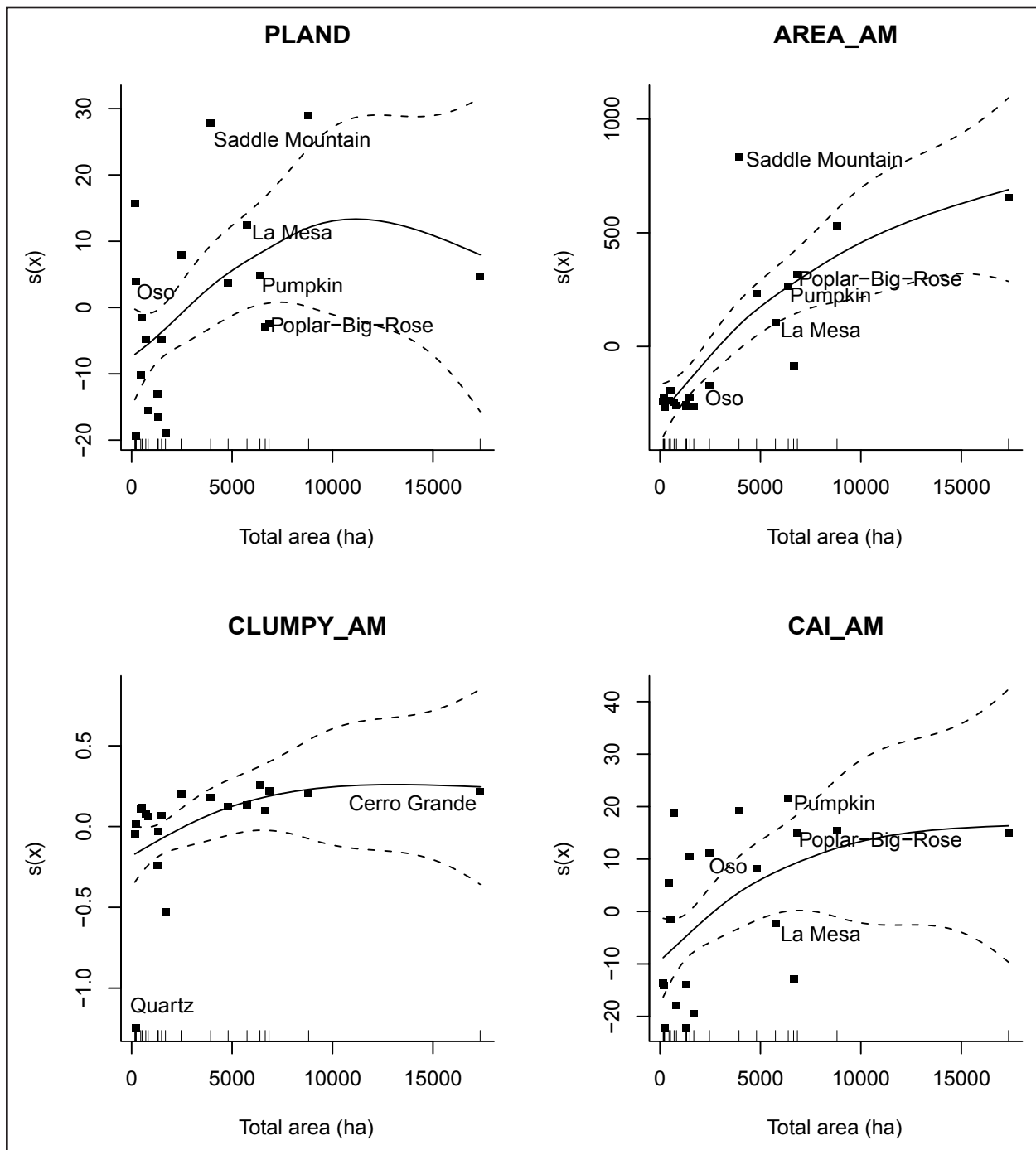


Figure 3. Plots of the GAM smooth functions for spatial pattern metrics that were generally related to fire size ($P < 0.2$). The y-axis is scaled by the smooth function of x . Dotted lines are 95% confidence intervals. Residuals are indicated with dots, and fire name labels are located at the lower right of the residual of interest, with the exception of Cerro Grande and Quartz. Although composition of burn severity (PLAND) and three aspects of burn severity configuration (AREA_AM, CLUMPY, and CAI_AM) generally increased with fire size, some fires deviated from this trend, e.g., the Saddle Mountain Fire.

rough terrain occurred along the edge of steep slopes that curve around flatter areas (i.e., scarp slopes or combs).

Fires that were similar in either climatic context or physiography did not necessarily exhibit comparable patterns across the gradient

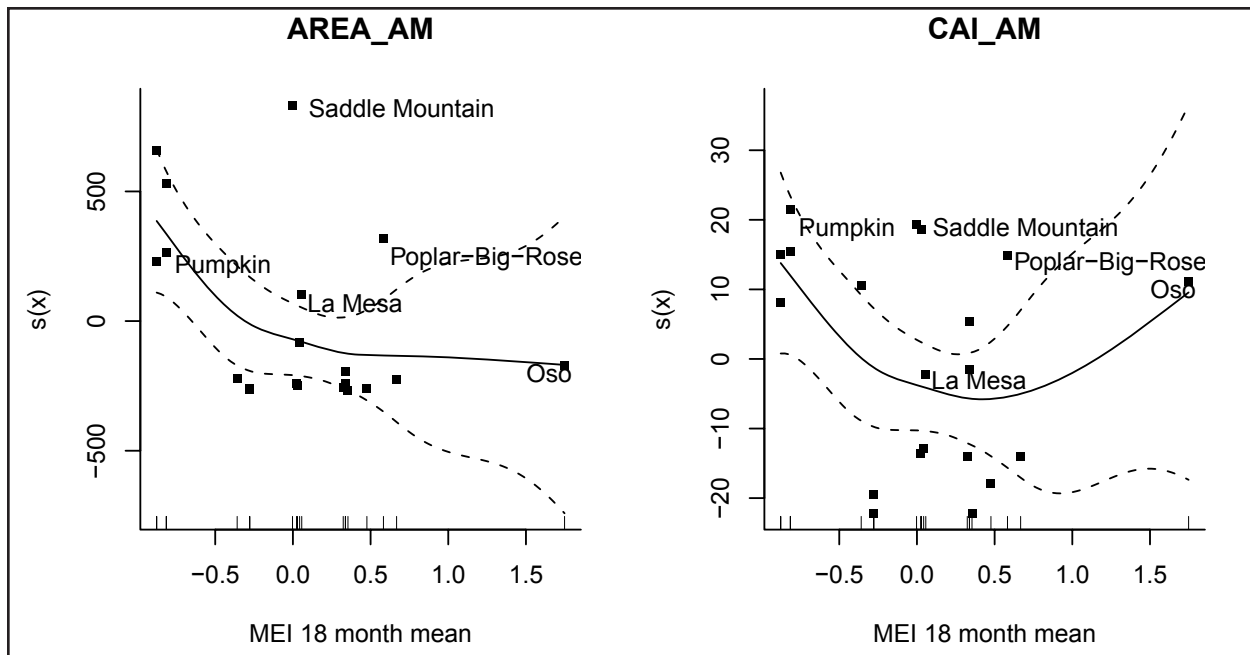


Figure 4. Plots of the GAM smooth functions for spatial pattern metrics that were related to variations in the MEI 18 month mean ($P < 0.2$). The y -axis is scaled by the smooth function of x . Dotted lines are 95% confidence intervals. Residuals are indicated with dots, and fire name labels are located at the lower right of the residual of interest, with the exception of Oso. Notable exceptions to overall trends include the Poplar-Big-Rose Fire, which had high AREA_AM and CAI_AM for a fire with its climate.

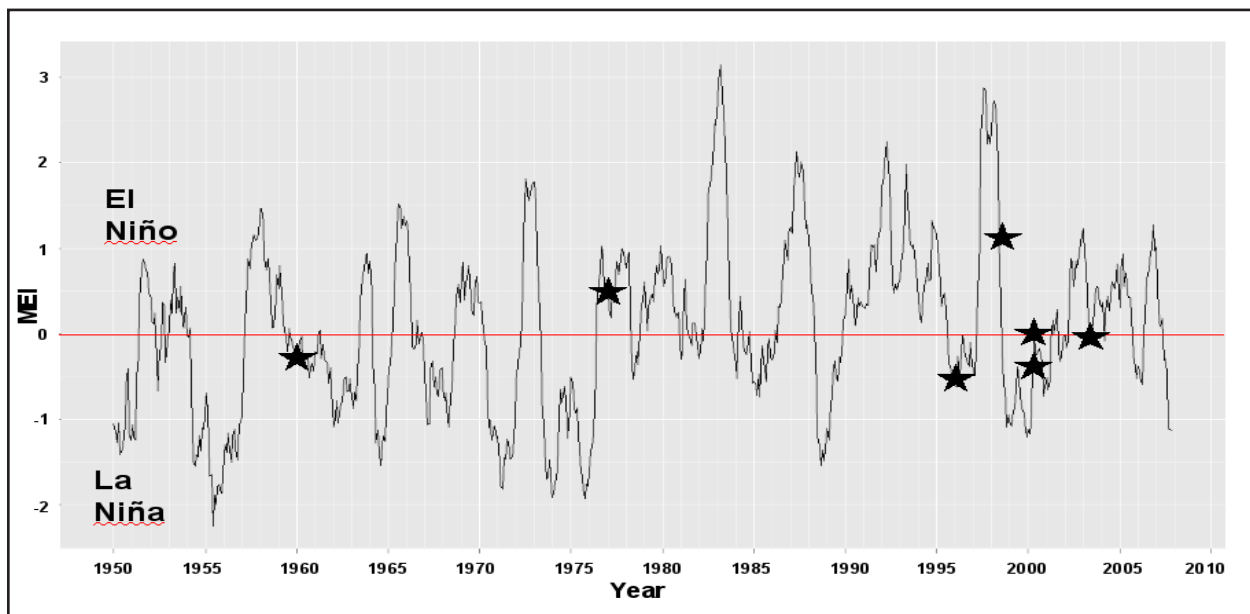


Figure 5. The approximate location of the nine fires included in the within-fires analysis on the MEI gradient, based on the MEI for the month the fire was detected. From left to right, starred locations correspond to Saddle Mountain (1960), La Mesa (1977), Dome (1996), and Oso (1998). Four fires in year 2000 were Cerro Grande and Outlet (MEI -0.34) and Pumpkin and Viveash (MEI 0.03), followed by Poplar-Big-Rose (2003).

in topographic complexity (Figure 6). For example, severity declined after a threshold was reached at fires with similarities in topography

but at opposite ends of the MEI gradient (Cerro Grande and Oso; Figure 6). The decline at Oso was influenced by few and scattered loca-

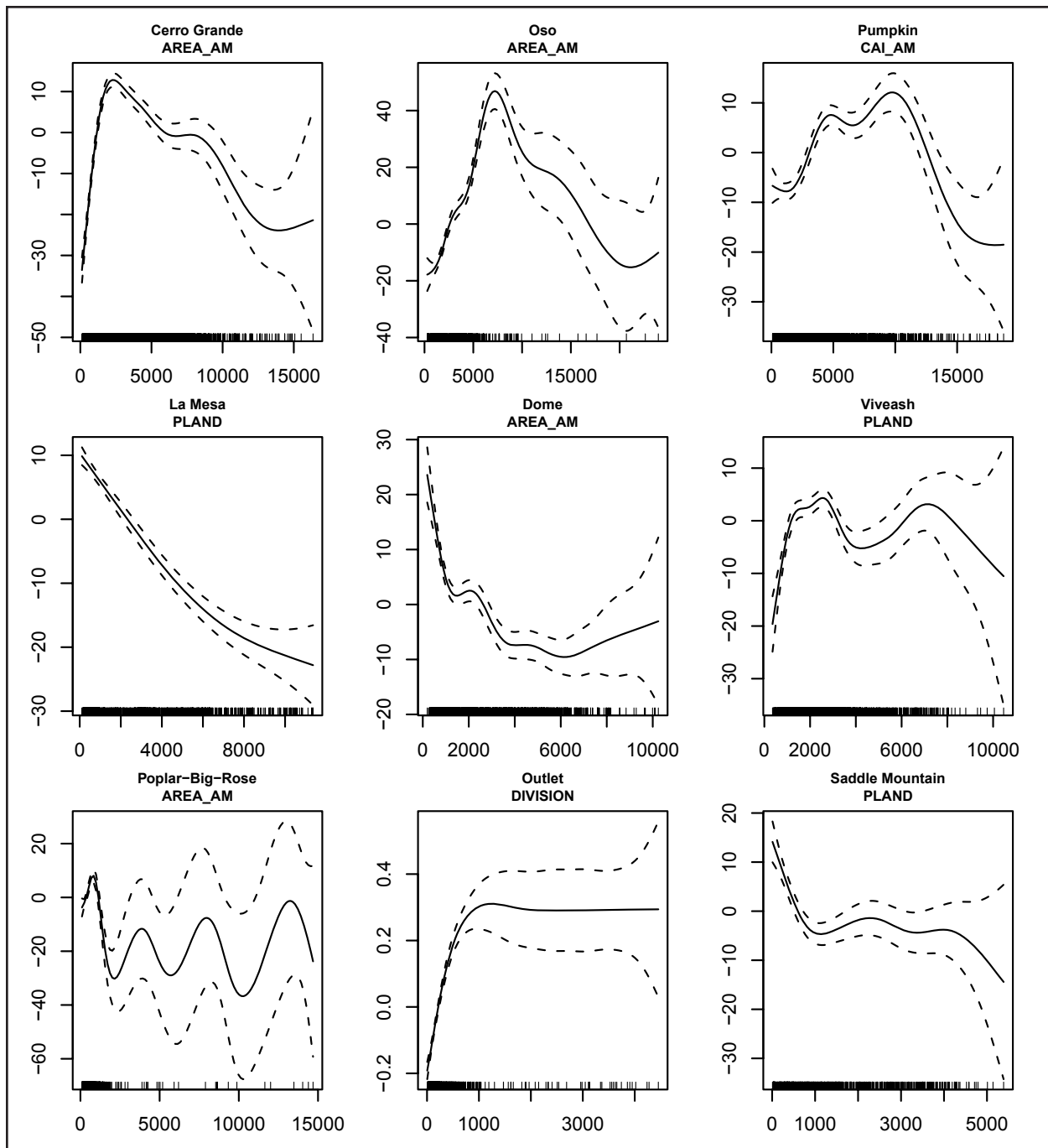


Figure 6. GAM smooth functions across the gradient in topographic complexity (shown on x-axis) at each of the nine fires. The y-axis is scaled by the smooth function of x , and dotted lines are 95% confidence intervals. Cerro Grande, Viveash, Pumpkin, Poplar-Big-Rose, and Oso exhibited an increase in severity with topographic complexity at the lower end of the gradient (focus on area with concentration of sample points, i.e., as indicated on the x-axis rug). Severity decreased only at the extreme end of the gradient at Pumpkin and Oso, where points were more scattered. Severity at Outlet, Saddle Mountain, Dome, and La Mesa generally decreased with topographic complexity, with some areas exhibiting no change at Outlet and Saddle Mountain. Note: increased values of DIVISION (Outlet graph) correspond to lower severity by definition.

tions at the high end of the gradient. Two other New Mexico fires, La Mesa and Dome, did not exhibit the initial upward trend in severity of Cerro Grande and Oso. La Mesa was the only fire that showed a consistent negative effect of topographic complexity on severity; the overall downward pattern in the Dome model included fluctuations across the gradient, with a few locations driving a final, upward trend.

Outlet and Poplar-Big-Rose, the Arizona fires with the most geographic similarity but diverse positions on the MEI gradient, showed downward trends over the region of the gradient with most data points (i.e., high density of points on the x -axis, Figure 6). Scattered locations across the remainder of the gradient resulted in a stable pattern at Outlet, and a widely-fluctuating pattern at Poplar-Big-Rose (note wider range of y -axis scale), which occurred in areas of high variability at the edge of the Grand Canyon. The increase in severity at low levels on the gradient observed at Oso and Cerro Grande appeared again at Poplar-Big-Rose.

The three fires with unique topographic characteristics but similar MEI context also differed in response patterns (Figure 6). At Pumpkin, severity increased until midway along gradient, at which point it declined steeply. Viveash exhibited widely fluctuating patterns until the highest end of the gradient, where its decline was influenced by scattered locations with extreme values. Saddle Mountain relationships were negative, and then stable, before a final negative turn.

DISCUSSION

Among-Fires Analysis

Our results led to three important findings at the scale of the 20 fires. First, relationships between the area burned by fires in the southwest and climate conditions, based on MEI, can include significant variability. For example, the Poplar-Big-Rose and Oso fires were

exceptionally large, given their El Niño position on the climate gradient (Figure 2). However, several of the larger fires in our study occurred as expected during the cool dry extremes of La Niña (i.e., year 2000), which often signals years of widely synchronous fires in the southwest (Swetnam and Betancourt 1998). The strong El Niño of 1997-1998 likely played a role by increasing fine fuel production in ponderosa pine forests where fuel conditions can limit or promote fire (Schoennegal *et al.* 2004).

The high level of variation we observed may be due to factors that are not necessarily related to MEI. Burning conditions, including wind, humidity, and temperature can inhibit or increase fire spread (Flannigan and Wotton 2001). In addition, the effects of La Niña-El Niño cycles can be intensified by teleconnections with broader-scale climate conditions (Baker 2003). Fires can become larger under favorable conditions, but landscape characteristics, as well as fire management may limit or increase area burned (Firefighters United for Safety, Ethics, and Ecology 2006; van Wageningen and Lutz 2007).

Second, spatial properties of fire severity were either unrelated or less clearly related to fire size. Exceptions to overall trends that resulted in weaker models were well-illustrated by the smooth plots (Figure 3). For example, two of the largest fires, Poplar-Big-Rose and Cerro Grande, did not conform to the trend of increasing high-severity composition with fire size (Figure 3). The moderate El Niño climate context of Poplar-Big-Rose could have influenced this outcome by creating moist fuels that were less conducive to fire spread over its approximately 60 days of burning (National Park Service 2003). In contrast, our model results indicated that topographic variability resulted in lower severity at some locations at Cerro Grande, an extreme La Niña fire. Aggregation of high-severity cells and patch division did not relate to fire size; however, size of patches gen-

erally increased with fire size (Figure 3). Larger overall size can accommodate larger patches, which in turn may include more core area.

Third, we did not find consistent trends in severity across the MEI climate gradient. The general decline in patch size toward wetter, El Niño climate was marked by several exceptions including Saddle Mountain and Poplar-Big-Rose (Figure 4). In addition, the Oso Fire had one of the larger values for core area, indicating that fuel and burning conditions were conducive to severe burning even at the warm moist end of the MEI gradient. Fires on the opposite end of MEI often included extreme burning conditions favorable to high-severity fire (e.g., the Pumpkin Fire; Forest Service 2000). But the hot temperatures and strong winds recorded during some portions of the Oso Fire (National Oceanic and Atmospheric Administration 1998) illustrate the need to better understand how burning conditions, in the timeframe of the fire event, are related to a wide range of broader-scale climate measured by the MEI.

It is also possible that climate measured at more local scales would be more correlated to fire severity. For example, metrics such as snowpack have been shown to relate to fire size (Lutz *et al.* 2009). Furthermore, correlations between climate and ecological phenomena have been shown to vary with the scale at which climate is measured (Peterson and Peterson 2001). Fluctuations in the El Niño Southern Oscillation (ENSO), including a major El Niño event in 1997-1998 (Wolter and Timlin 1998) and widespread drought (early 1950s and 2000s), provided a useful backdrop for describing variability in fire size and severity of our 20 fires. However, models with greater predictive ability might be achieved by quantifying relationships between severity and changes in snowpack, temperature, and short-term burning conditions.

Within-Fires Analysis

A major finding of our analysis was that topographic complexity affected severity not only during moderate climates, as predicted, but at some times and places within all of the nine fires (Figure 6). This was true for fires during a major drought year (e.g., Cerro Grande and Pumpkin), as well as fires that burned during wetter years (e.g., La Mesa and Poplar-Big-Rose). We were able to identify trends in the data by using a flexible modeling approach, which also proved advantageous in determining the direction of relationships between severity and terrain characteristics along the gradient of topographic complexity.

At low to moderate levels of topographic complexity, the direction of relationships differed between fires. In our topographic model, these levels corresponded to areas that range from flat to moderately sloping. In fire behavior models, fire spread has been shown to increase on gentle and even steep slopes by pre-heating fuels and increasing flame length (Rothermel 1983). At some fires, then, fire spread and fire severity apparently increased together at low to moderate levels of terrain complexity (including Cerro Grande, Oso, Pumpkin, Viveash, and Poplar-Big-Rose; Figure 6). But at other fires, fire severity decreased across the low to moderate range of our topographic gradient (La Mesa, Dome, Outlet, and Saddle Mountain; Figure 6). La Mesa was the only fire that exhibited a consistent, monotonic trend in severity across the topographic gradient, even during high winds and hot temperatures (Foxy 1984). Thus, locations where topography is conducive to fire spread may not produce increased severity.

In addition, we identified thresholds at which the direction of relationships across the topographic gradient changed. Our work represents a first step in quantifying the magnitude of change and the environmental conditions that define these non-linear responses,

meeting a recognized need for both research and management (Sonderregger *et al.* 2009). Understanding the range of conditions over which severity changes within large fires is needed to refine spatial models of fire-succession dynamics. Most models currently in use do not include measurements of terrain that explain significant amounts of variation in outcome (Cary *et al.* 2006). Our results suggest that experimentation with threshold relationships could prove useful in modeling efforts.

Within our study sites, abrupt shifts in severity often occurred beyond the low to moderate range of complexity (Figure 6). Once a threshold occurred, fire severity either decreased (Cerro Grande, Oso, Pumpkin, Poplar-Big-Rose) or remained unchanged (Dome, Viveash, Outlet, Saddle Mountain) across the middle to upper levels of topographic complexity (Figure 6). Where severity decreased, rougher terrain could either represent direct barriers to spread, or local environmental constraints on flammability and fuel continuity (Kellogg *et al.* 2008). In places where severity remained unchanged, variability in terrain was sometimes low (e.g., Outlet), but extreme burning conditions could have played a role in creating a lack of clear relationship (e.g., Dome and Viveash). Further study is required to unravel key factors at these thresholds of change under diverse climatic and geographic situations.

Management Implications

Managers who work in a particular forest must deal with the variability in fire characteristics that often deviate from averages taken across longer timeframes and large regions (Swetnam and Betancourt 1998). Understanding variability can provide important evidence for interpreting the non-equilibrium conditions that may accompany climate change (Wallington *et al.* 2005). Furthermore, to benefit forest management, the relevance of spatial patterns

of fire severity must be judged relative to qualitative changes in ecological processes. That is, how does spatial patterning of severity encourage or inhibit particular functions?

For example, using a simple analysis of spatial patterns of severity and knowledge of seed dispersal capabilities (e.g., Clark and Ji 1995), managers could identify particular areas where distances from legacy seed sources exceed dispersal capabilities. The influence of distance to seed source on regeneration of ponderosa pine and other species has been shown to persist for decades (Coop and Schoettle 2009; S.L. Haire, University of Massachusetts, unpublished data). Although patch size or high severity composition has been emphasized in forecasting fire effects (e.g., Lutz *et al.* 2009), patch configuration is more critical for seed dispersal; patches of large size can range from fairly circular to long and narrow. Similarly, spatial patterns that define connectivity for hydrological processes can be useful in predicting secondary fire effects (e.g., storm runoff; Moody *et al.* 2007). Identifying wildlife habitat for species of concern also benefits from consideration of patch configuration and edge effects defined by spatial patterns of fire severity at relevant scales (e.g., Kotliar *et al.* 2008, Roberts *et al.* 2008).

Finally, as the fire regime in the southwest evolves in relation to climate change, examination of effects for individual fire events in local management areas could lead to identification of climate contexts in which fires can produce an acceptable range of ecological effects. Data from fires that burn naturally (e.g., at Grand Canyon National Park) are especially valuable for building connections between fire size, severity, and climate. The Poplar-Big-Rose Fire, which occurred in a moderate La Niña climate (Figure 5), met natural resource objectives within study plots that were visited before and after the fire (Fulé and Laughlin 2007). Understory effects were commonly observed and fire-resistant species, including

ponderosa pine, persisted with low rates of mortality. A synthesis of information on forest composition, history of burning, antecedent climate, and fire effects will contribute to in-

creased opportunities for burns that meet management objectives but would otherwise be unwisely suppressed.

ACKNOWLEDGEMENTS

Thanks to J. Stone for photographic interpretation and mapping, and also to W.H. Romme, S. deStefano, C. Miller, and two anonymous reviewers for critical review and discussion. K. Bealey, E. Gdula, B. Higgins, S. Howard, C. Key, and P. Pope helped with data acquisition and mapping. Funding for the project was provided by The Nature Conservancy, US Geological Survey, University of Massachusetts, and a fellowship from the American Association of University Women.

LITERATURE CITED

- Baker, W.L. 2003. Fires and climate in forested landscapes of the US Rocky Mountains. Pages 120-157 in: T.T. Veblen, W.L. Baker, G. Montenegro, and T. Swetnam, editors. Fire and climatic change in temperate ecosystems of the western Americas. Springer-Verlag, New York, USA.
- Cary, G.J., R.E. Keane, R.H. Gardner, S. Laval, M.D. Flannigan, I.D. Davies, L. Chao, J.M. Lenihan, S. Ruppert, and F. Mouillot. 2006. Comparison of the sensitivity of landscape-fire-succession models to variation in terrain, fuel pattern, climate and weather. *Landscape Ecology* 21: 121-137.
- Clark, J.S., and Y. Ji. 1995. Fecundity and dispersal in plant-populations—implications for structure and diversity. *American Naturalist* 146: 72-111.
- Collins, B.M., M. Kelly, J.W. van Wagtenonk, and S.L. Stephens. 2007. Spatial patterns of large natural fires in Sierra Nevada wilderness areas. *Landscape Ecology* 22: 545-557.
- Coop, J.D., and A.W. Schoettle. 2009. Regeneration of Rocky Mountain bristlecone pine (*Pinus aristata*) and limber pine (*Pinus flexilis*) three decades after stand replacing fires. *Forest Ecology and Management* 257: 893-903.
- De'ath, G., and K.E. Fabricius. 2000. Classification and regression trees: a powerful yet simple technique for the analysis of complex ecological data. *Ecology* 81: 3178-3192.
- Fire Fighters United for Safety, Ethics, and Ecology. 2006. Scorched earth tactics: backfires and burnouts. < <http://www.fusee.org> >. Accessed 27 January 2009.
- Flannigan, M.D., and B.M. Wotton. 2001. Climate, weather, and area burned. Pages 351-373 in: E.A. Johnson and K. Miyanishi, editors. Forest fires: behavior and ecological effects. Academic Press, San Diego, California, USA.
- Foxx, T.S. 1984. Description of La Mesa Fire. Pages 1-10 in: T.S. Foxx, editor. La Mesa Fire Symposium. Los Alamos National Laboratory Report, LA-9236-NERP, New Mexico, USA.
- Fulé, P.Z., and D.C. Laughlin. 2007. Wildland fire effects on forest structure over an altitudinal gradient, Grand Canyon National Park, USA. *Journal of Applied Ecology* 44: 136-146.
- Grissino-Mayer, H.D., and T.W. Swetnam. 2000. Century-scale climate forcing of fire regimes in the American southwest. *Holocene* 10: 213-220.

- Guisan, A., T.C. Edwards, Jr., and T. Hastie. 2002. Generalized linear and generalized additive models in studies of species distributions: setting the scene. *Ecological Modelling* 157: 89-100.
- Haire, S.L., and K. McGarigal. 2008. Inhabitants of landscape scars: succession of woody plants after large, severe forest fires in Arizona and New Mexico. *The Southwestern Naturalist* 53: 146-161.
- Kellogg, L.K.B., D. McKenzie, D.L. Peterson, and A.E. Hessler. 2008. Spatial models for inferring topographic controls on historical low-severity fire in the eastern Cascade Range of Washington, USA. *Landscape Ecology* 23: 227-240.
- Key, C.H. 2006. Ecological and sampling constraints on defining landscape fire severity. *Fire Ecology* 2(2): 34-59.
- Key, C.H., and N.C. Benson. 2005. Landscape assessment: ground measure of severity, the Composite Burn Index, and remote sensing of severity, the Normalized Burn Ratio. In FIRE-MON: Fire Effects Monitoring and Inventory System. USDA Forest Service General Technical Report RMRS-GTR-164-CD:LA1-51. <<http://www.fire.org/firemon/>>. Accessed 27 January 2009.
- Kotliar, N.B., E.W. Reynolds, and D.H. Deutschman. 2008. American three-toed woodpecker response to burn severity and prey availability at multiple spatial scales. *Fire Ecology* 4(2): 26-45.
- Littell, J.S., D. McKenzie, D.L. Peterson, and A.L. Westerling. In press. Climatic influences on twentieth-century area burned in ecoprovinces of the western US. *Ecological Applications*.
- Lutz, J.A., J.W. van Wagtenonk, A.E. Thode, J.D. Miller, and J.F. Franklin. 2009. Climate, lightning ignitions, and fire severity in Yosemite National Park, California, USA. *International Journal of Wildland Fire* 18(6): in press.
- Margolis, E.Q., T.W. Swetnam, and C.D. Allen. 2007. A stand-replacing fire history in upper montane forests of the southern Rocky Mountains. *Canadian Journal of Forest Research* 37: 2227-2241.
- McGarigal, K., S.A. Cushman, M.C. Neel, and E. Ene. 2002. FRAGSTATS: Spatial pattern analysis program for categorical maps. University of Massachusetts, Amherst. <<http://www.umass.edu/landeco/research/fragstats/fragstats.html>>. Accessed 27 January 2009.
- Miller, C., M.-A. Parisien, A.A. Ager, and M.A. Finney. 2008. Evaluating spatially-explicit burn probabilities for strategic fire management planning. *Transactions on Ecology and the Environment* 119: 245-252.
- Moody, J.A., D.A. Martin, S.L. Haire, and D.A. Kinner. 2007. Linking runoff response to burn severity after a wildfire. *Hydrological Processes* 22: 2063-2074.
- National Park Service-US Geological Survey 2007. National Burn Severity Mapping Project. <<http://burnseverity.cr.usgs.gov>>. Accessed 27 January 2009.
- National Park Service. 2003. Poplar fire. <www.nps.gov/archive/grca/media/2003/2oct03.htm>. Accessed 15 November 2008.
- National Oceanic and Atmospheric Administration. 1998. National weather service. <<http://www.nws.noaa.gov>>. Accessed 15 November 2008.
- National Oceanic and Atmospheric Administration. 2009. Climate indices. <<http://www.cdc.noaa.gov/ClimateIndices>>. Accessed 30 June 2008.
- Peterson, D.W., and D.L. Peterson. 2001. Mountain hemlock growth responds to climatic variability at annual and decadal time scales. *Ecology* 82: 3330-3345.

- Pickett, S.T.A., V.T. Parker, and P. Fielder. 1992. The new paradigm in ecology: implications for conservation biology above the species level. Pages 65-88 in: P. Fielder and S. Jain, editors. *Conservation biology: the theory and practice of nature conservation*. Chapman and Hall, New York, New York, USA.
- Roberts, S.L., J.W. van Wagtenonk, A.K. Miles, D.A. Kelt, and J.A. Lutz. 2008. Modeling the effects of fire severity and spatial complexity on small mammals in Yosemite National Park, California. *Fire Ecology* 4(2): 83-104.
- Romme, W.H., E.H. Everham, L.E. Frelich, M.A. Moritz, and R.E. Sparks. 1998. Are large, infrequent disturbances qualitatively different from small, frequent disturbances? *Ecosystems* 1: 524-534.
- Rothermel, R.C. 1983. How to predict the spread and intensity of forest and range fires. USDA Forest Service General Technical Report INT-143. Ogden, Utah, USA.
- Schoennagel, T., T.T. Veblen, and W.H. Romme. 2004. The interaction of fire, fuels, and climate across Rocky Mountain forests. *Bioscience* 54: 661-676.
- Sonderegger, D.L., H. Wang, W.H. Clements, and B.R. Noon. 2009. Using SiZer to detect thresholds in ecological data. *Frontiers in Ecology and Environment* 7(4): 190-195.
- Stambaugh, M.C., and R.P. Guyette. 2008. Predicting spatio-temporal variability in fire return intervals using a topographic roughness index. *Forest Ecology and Management* 254: 463-473.
- Swetnam, T.W., and J.L. Betancourt. 1998. Mesoscale disturbance and ecological response to decadal climatic variability in the American southwest. *Journal of Climate* 11: 3128-3147.
- Turner, M.G., R.H. Gardner, and R.V. O'Neill. 2001. *Landscape ecology in theory and practice*. Springer-Verlag, New York, New York, USA.
- Turner, M.G., and W.H. Romme. 1994. Landscape dynamics in crown fire ecosystems. *Landscape Ecology* 9: 59-77.
- US Geological Survey. 1999. National elevation dataset. <<http://www.ned.usgs.gov>>. Accessed 27 January 2009.
- van Wagtenonk, J.W., and J.A. Lutz. 2007. Fire regime attributes of wildland fires in Yosemite National Park, USA. *Fire Ecology* 3(2): 34-52.
- Wallington T.J., R.J. Hobbs, and S.A. Moore. 2005. Implications of current ecological thinking for biodiversity conservation: a review of the salient issues. *Ecology and Society* 10. <<http://www.ecologyandsociety.org/vol10/iss1/art15/>>. Accessed 15 November 2008.
- Westerling, A.L., H.G. Hidalgo, D.R. Cayan, and T.W. Swetnam. 2006. Warming and earlier spring increase western US forest wildfire activity. *Science* 313: 940-943.
- White, P.S., and S.T.A. Pickett. 1985. Natural disturbance and patch dynamics: an introduction. Pages 3-13 in: S.T.A. Pickett and P.S. White, editors. *The ecology of natural disturbance and patch dynamics*. Academic Press, New York, New York, USA.
- Whitlock, C. 2004. Forests, fires and climate. *Nature* 432: 28-29.
- Wolter, K., and M.S. Timlin. 1998. Measuring the strength of ENSO events: how does 1997/98 rank? *Weather* 53: 315-324.
- Wood, S.N. 2006. *Generalized additive models: an introduction with R*. Chapman and Hall, Boca Raton, Florida, USA.
- Yang J., H.S. He and S.R. Shifley. 2008. Spatial controls of occurrence and spread of wildfires in the Missouri Ozark Highlands. *Ecological Applications* 18(5): 1212-1225.